

A H Botha for the NAC staff*

Abstract

The National Accelerator Centre (NAC) is at present being established around a 200 MeV separated-sector cyclotron and an 8 MeV solid-pole injector cyclotron. The design of the SSC magnets has been finalised and tenders for the manufacture of the magnet steel have recently been received. Detailed designs of the central region of the SSC, the magnet vacuum chambers, main coils and the magnet supports have been made. The general layout of the accelerator vaults and adjacent experimental areas have been frozen. Consultant engineers, architects and quantity surveyors have been appointed and initial planning for the building and services has been completed. Final design of the accelerator building is now under way. Progress on these aspects of the project and its present status are reported.

Introduction

The proposal for a multidisciplinary accelerator facility presented at the previous international cyclotron conference¹ and elsewhere^{2,3} has been approved. A National Accelerator Centre (NAC) has been created within the framework of the Council for Scientific and Industrial Research who will take responsibility for the erection and operation of the Centre. The NAC will form a service facility for all universities and research groups in the country.

While initial funding was limited, increasing funds have been made available in each succeeding year. The rate of funding is to some extent reflected in the growth of the NAC personnel, as shown in figure 1.

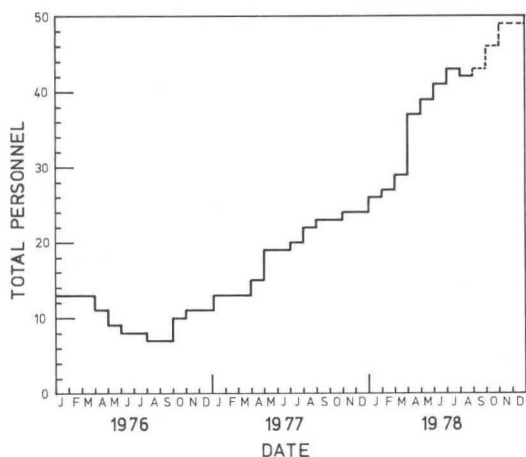


Fig. 1: Growth of NAC personnel

The accelerator complex will house a variable-energy, separated-sector cyclotron with a K-value of 200 MeV and a solid-pole, injector cyclotron with a K-value of 8 MeV. For heavier ions, a second injector with a 40 MeV K-value is planned. Both light and heavy ion beams will ultimately be available for nuclear physics and related disciplines, while intense beams of light ions with energies up to 100 MeV/nucleon will be provided for radiotherapy and isotope production.

After extensive geological and geophysical studies of a number of possible sites, a suitable site has been

selected, adjacent to the Southern Universities Nuclear Institute where a CN van de Graaff accelerator is in operation.

General Layout and Beam Transport

The general layout of the facility is shown in fig. 2, although the exact location of the heavy-ion injector has not yet been determined. The experimental area remains unchanged from the design reported earlier³ but the beam now goes directly from the SSC to the radiotherapy area. This allows room for three possible isocentric therapy units. The isotope production area is to one side, the beam being switched there by a low-field dipole M3. Two isotope vaults are planned.

The transfer beamline between SPC1 and the SSC is separated into various sections with independent functions. The first quadrupole triplet forms a double waist, after which the beam is made achromatic by the symmetric system comprising two 45° dipoles with doublets before, between and after them. Energy selection can be done at a slit at the midpoint of this system. The achromatic beam is then bunched to produce a minimum pulse length at the first SSC valley. The resulting increase in momentum spread is small because the buncher is approximately midway along the transfer line. After the buncher we have a beam-shaping section consisting of six quadrupoles in an orthogonal system i.e. with horizontal and vertical waists at alternate quadrupoles so that the size of the final waists in x and y may be controlled independently⁴.

The 11° dipole again introduces dispersion which is controlled by the next four quadrupoles so that the dispersed rays are injected correctly for optimal acceleration. The beam then passes through the stray field of the sector magnets (which bends it by approximately 4°), through two dipoles and a magnetic inflection channel. The six-dimensional eigen-ellipse on the valley midline at injection radius has been calculated using the transfer matrix of the first equilibrium orbit. The transfer beamline is tuned to produce this required beam ellipse.

The extracted beam is directed past the sector magnet by two dipoles (M1 and M2). These are separated by a quadrupole triplet and followed by a doublet to achieve an achromatic double waist at M3. The section from M3 to slit S1 (common to the therapy and experimental lines) is used to shape the beam in an orthogonal system.

From S1 the therapy line passes through a telescopic quadrupole system and a switching magnet (SWT) followed by another telescopic system (which may consist of two quadrupole doublets rather than two triplets⁴), and a final triplet before entering one of the three radiotherapy systems. Each isocentric system consists of three dipoles (which rotate about the axis of the preceding quadrupoles) with edge angles designed to produce a near-achromatic symmetric beam on target for all angles of rotation⁴.

The double-monochromator (S1 to SR1) is unchanged from the previous design², but the telescopic system (SR1 to SWR) has been modified to allow vertical magnifications greater than unity whilst retaining unit horizontal magnification⁴. This permits a smaller gap height for the 90° dipoles MP1 and MP2.

The Light-Ion Injector Cyclotron

The light-ion injector will deliver high-intensity beams of light ions with a maximum proton energy of 8 MeV.

*National Accelerator Centre
Council for Scientific and Industrial Research
P O Box 320, Stellenbosch, South Africa.

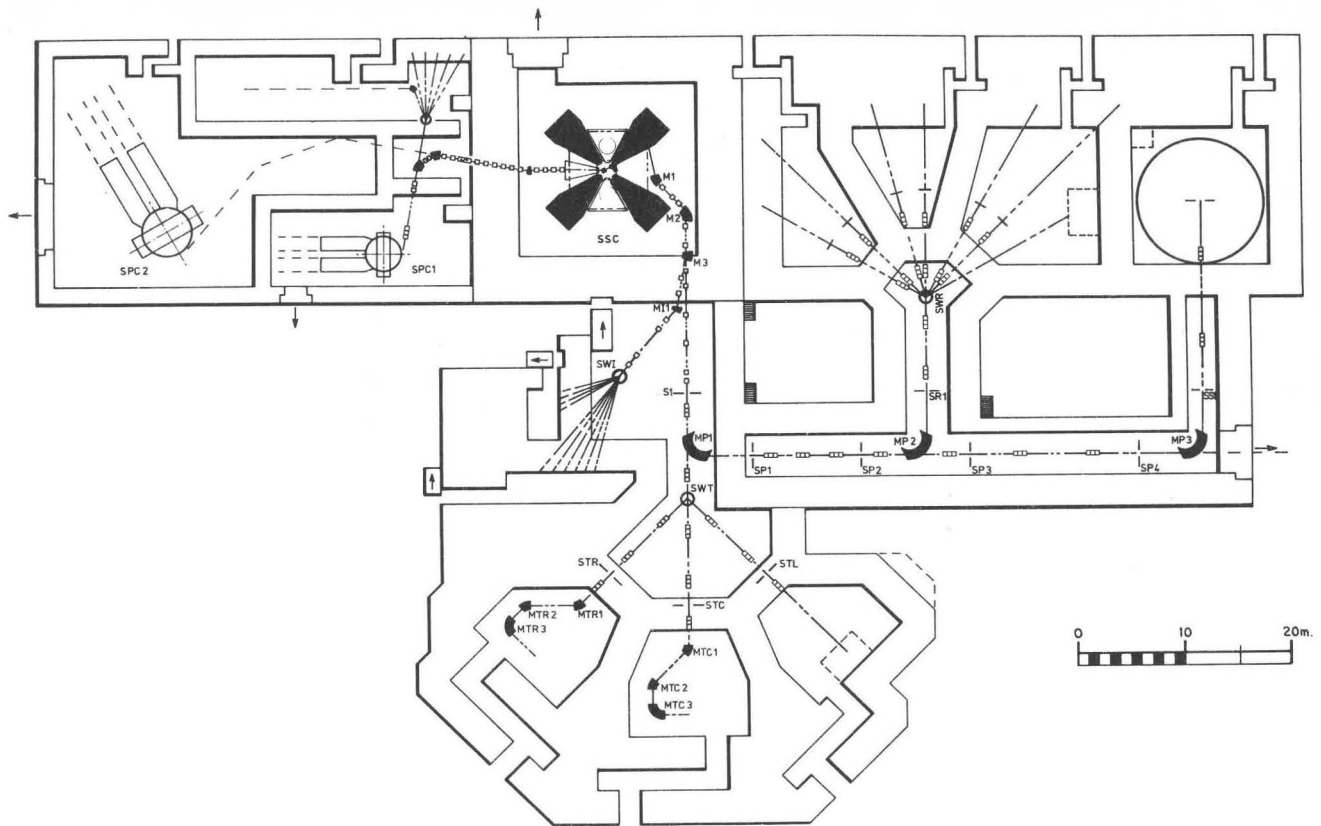


Fig. 2: Layout of the shielded areas showing cyclotrons and beamlines

In order to simplify the design of the central region and the extraction system, the injector will be operated in a constant-orbit mode for most particles and particle energies.

The main characteristics of the injector are summarised in table 1.

Table 1: Characteristics of the Light-ion Injector

K-value	8 MeV
Magnet Sectors	$4 \times 45^\circ$
Magnetic Flux Density	0,86 T
Extraction Radius	47,6 cm
Pole Gap on Hill	15 cm
Pole Gap in Valley	25 cm
Frequency Range	7,5 - 26 MHz
Harmonic Numbers	2 and 6
Dees	$2 \times 90^\circ$
RF Power Consumption	$2 \times 17,5$ kW

Various extraction schemes have been studied. It is possible to extract the beam with a single electrostatic channel followed by a magnetic channel. An electrostatic field strength of 70 kV/cm will be used whereas a flux density of 0,15 Tesla and a gradient of 5 Tesla/m will be required for the magnetic channel. These components will be designed to have acceptances of more than 160 mrad in both the horizontal and vertical directions.

Because of the small size of the dees the total dee capacitance is small, and relatively long (4 m) resonators are required for the rf system. Ways of increasing the total dee capacitance are being investigated. After study of the main components, the possibility of having this machine manufactured commercially is at present

being investigated.

The Separated-Sector Cyclotron

The main components of the SSC are shown in figure 3. Four sector magnets, four magnet vacuum chambers, two delta-type resonators and two valley chambers are shown. The beam is brought into the cyclotron by means of two bending magnets and a magnetic inflection channel. For extraction an electrostatic channel, two septum magnets and a bending magnet are employed.

Magnets and Magnet Vacuum Chambers

The SSC has four identical C-shaped magnets. A sector angle of 34° was chosen to prevent crossing the $\nu_z = 1$ and $2\nu_z + \nu_x = 4$ resonances for both light and heavy ions.

In the pole gap of each of the magnets a sector-shaped vacuum chamber will be installed. A cross-sectional view of the poles, trim coils and vacuum chamber is shown in figure 4. The vacuum chamber will be supported from the poles by 96 bolts. The considerations which led to this design are described in detail elsewhere in these proceedings⁵. The main advantage of this form of construction is that the main and trim coils as well as the pole faces are outside the vacuum chamber and cannot contribute to outgassing.

The influence of the vacuum chamber material in the pole gap and the holes through the pole-pieces have been investigated. Measurements of the permeability of AISI 310 stainless steel showed that the material of the vacuum chamber will introduce field perturbations of less than 0,25 percent. Perturbations of the same order of magnitude are introduced by the holes in the pole-pieces but can be corrected by using ferromagnetic

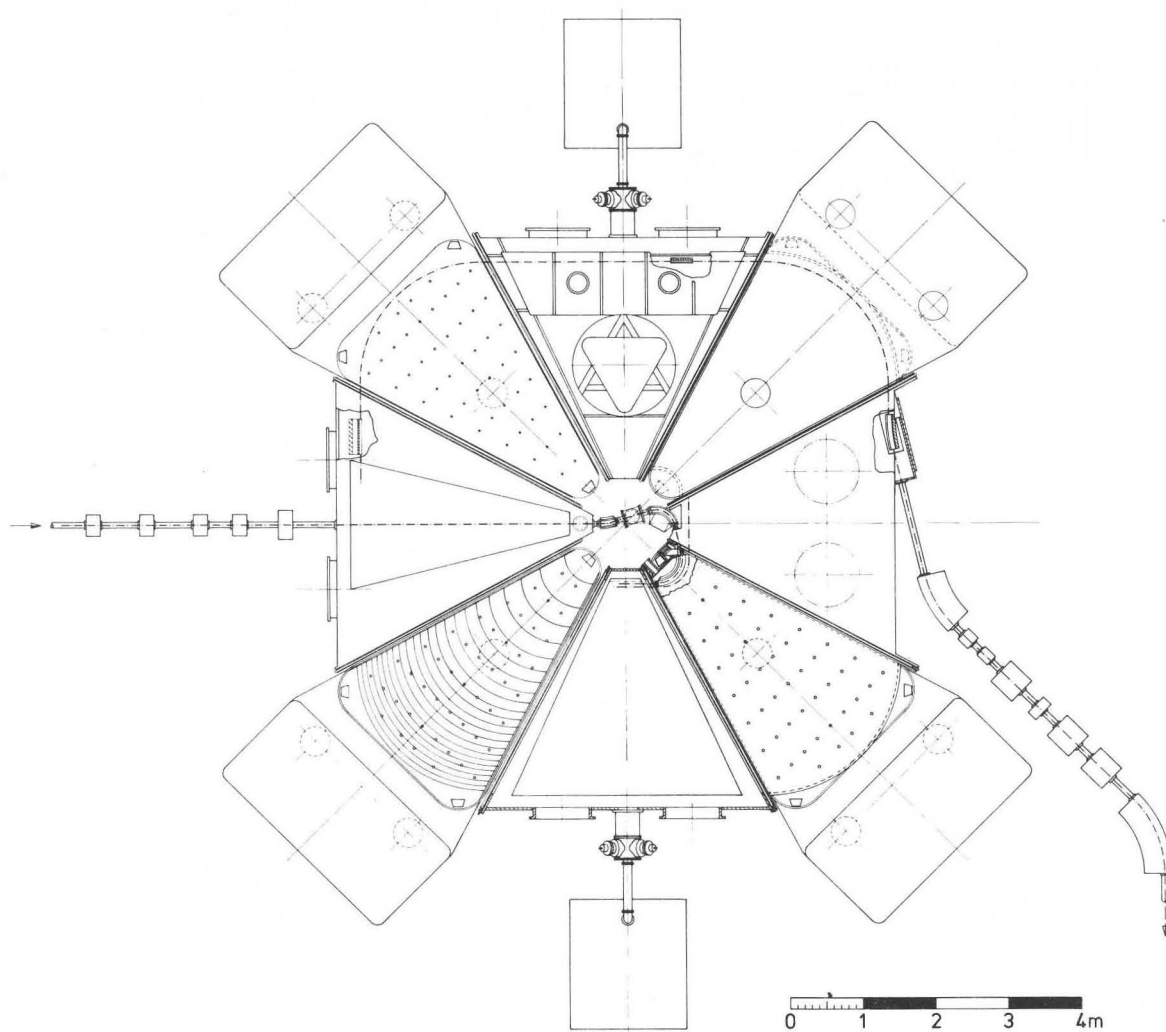


Fig. 3: Layout of the separated-sector cyclotron

washer-shaped shims around each bolt. The estimated effect on the beam by the resultant field perturbations is negligible.

The deflection of the magnets and the magnet vacuum chambers under the magnetic attractive force between the poles and forces on the vacuum chamber due to air pressure were analysed using finite element methods.

Detailed designs of the magnets, magnet vacuum chambers, main coils and supports have been realised. Tenders for manufacture of the magnet steel have been received and negotiations for the manufacture of the magnet vacuum chambers finalised. Arrangements for the manufacture of the main coils, supports and the main power supply for the magnets are in progress.

Orbit Calculations

The recent developments in our beam orbit calculations are associated with the fact that numerical data of realistic magnetic fields had become available. These data consisted of values of the field at the nodes of a cylindrical grid in the median plane, and had been obtained by means of accurate field calculations rather than from measurements on models of the magnets. The fineness of the grid was limited by the time and storage requirements of the programs calculating the field. In the case of the SSC field calculations, radial and azimuthal grid spacings Δr and $\Delta\theta$ of 73 mm and 1° were used. Since both Δr and $r\Delta\theta$ at large radii were larger

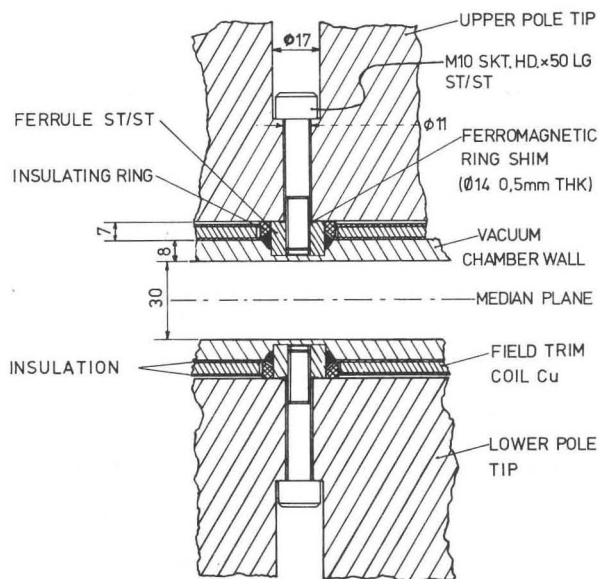


Fig. 4: Section of SSC magnet showing method of support of vacuum chamber.

than the pole gap (60 mm), the magnetic field at the magnet edges varied rapidly, i.e. changed by large amounts from one grid point to the next. This rapid variation of the field caused difficulties with several of the numerical techniques.

Firstly, conventional techniques of calculating the derivatives of the field (e.g. $\partial B/\partial r$ or $\partial B/\partial \theta$) gave unsatisfactory results. Cubic splines collocating with the radial distribution values (from which $\partial B/\partial r$ would normally be calculated) tended to oscillate strongly about the field values in the vicinity of the field edges. Similarly, conventional Fourier analysis of the azimuthal distribution and subsequent reconstitution of a smoothed field from the Fourier expansion formula with Lanczos factors included, had the effect of smearing out the field edges. A technique was therefore developed to calculate derivatives of such rapidly varying fields more accurately: it consists of fitting a suitable function $f(x)$ (where x represents r or θ) to the (radial or azimuthal) distribution B_i in such a way that the difference $B_i - f_i$ varies smoothly with x . A suitable function for our edge field is:

$$f(x) = \left(\sum_{j=0}^m a_j x^j \right) [1 + e^{\alpha(x-\bar{x})}]^{-1}$$

where $\alpha = \alpha_0 + \frac{2}{\pi} \beta \tan^{-1}[\gamma(x-\bar{x})]$

In practice the coefficients a_j and the parameter γ are determined directly from the distribution, and only α_0 , β and \bar{x} varied in a least-squares fit of $f(x)$ to the data B_i . The resulting difference distribution $B_i - f_i$ varies slowly and a cubic spline fits smoothly to it. The derivatives of B_i are calculated as a sum of the derivatives of the analytical function and the spline function. In figures 5 and 6 are shown typical radial and azimuthal distributions, the analytical functions fitted to them, and the difference distribution $B_i - f_i$. Derivatives calculated by this method proved to be far more accurate than with the previous techniques.

A second difficulty caused by the rapid variation of the field occurred during numerical integration of the

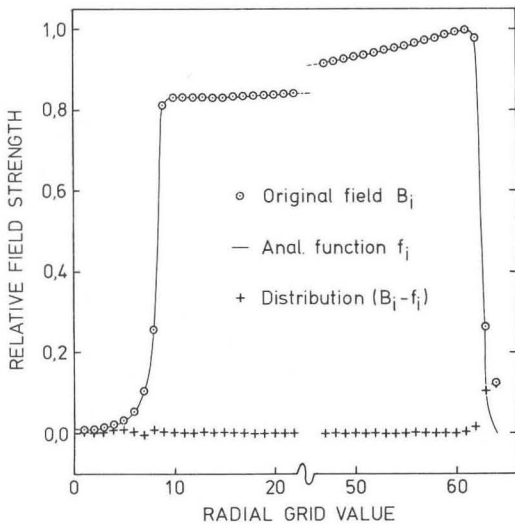


Fig. 5: Radial field distribution B_i and fitted analytical function f_i .

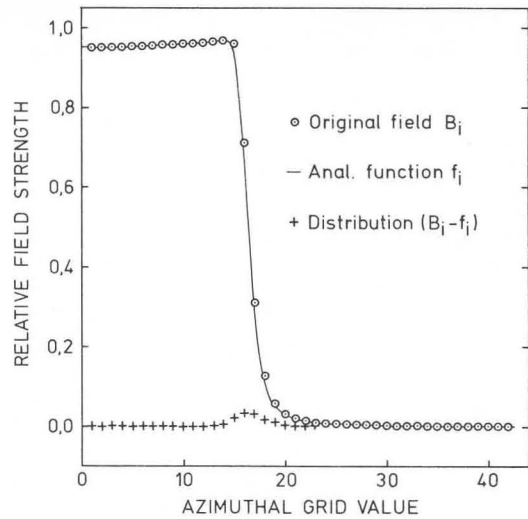


Fig. 6: Azimuthal field distribution B_i and fitted analytical function f_i .

differential equations of motion. The program in question employed the Milne linear 4-step predictor-corrector method, although the results hold more generally for any integration method derived by truncation of an infinite series. A calculation of estimated local truncation errors of the ($k=4$) Milne method showed that large errors were being made by the integration routine in the vicinity of the azimuthal field edges, because the 5th (= $k+1$ th) differences of the azimuthal distribution did not vanish in the vicinity of the field edge, but remained large. The only practical solution was to decrease the step-size to $\frac{1}{4}^\circ$, for which the local truncation errors were acceptably low.

After the abovementioned problems had been solved we were able to calculate the linear focussing properties of the SSC for a number of representative ions and energies. The results are shown in figure 7.

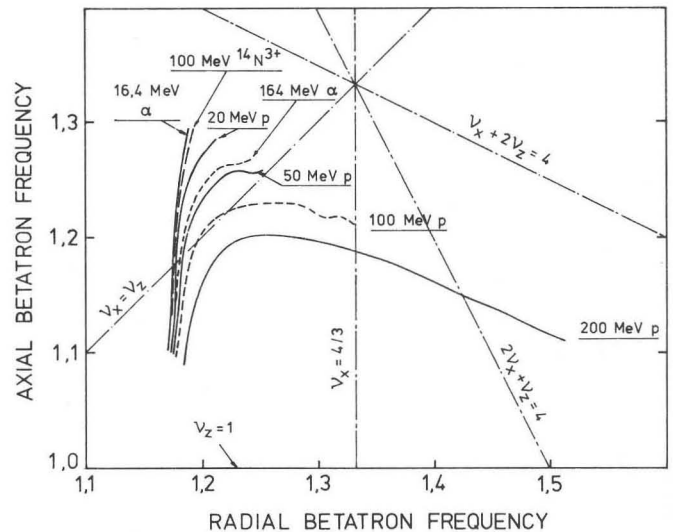


Fig. 7: Operating curves in ν_x, ν_z space

Vacuum System

The SSC requires a vacuum in the low 10^{-5} Pa region to ensure a high percentage transmission for heavy ion beams. For light ion beams an operating pressure in the

low 10^{-4} Pa region would be adequate.

The vacuum chamber of the SSC will be of a modular construction and will consist of eight separate chambers sealed at their interfaces by means of expanding seals similar to those in use at SIN. The volume and area of the chamber with its components will be about 50 m^3 and 500 m^2 respectively. The total gas load has been estimated to be $3 \times 10^{-3} \text{ Pa}\cdot\text{m}^3\cdot\text{s}^{-1}$. Leakage and outgassing of metal surfaces and elastomers contribute 10%, 20% and 70% respectively to this value. The elastomer seals are the major contributors to the total gas load and attempts will therefore be made to reduce the gas load from seals by reducing their number and making use of metal seals, feather welds and guard vacuums where possible. To reduce the pressure in the SSC to 1×10^{-5} Pa with an estimated gas load of $3 \times 10^{-3} \text{ Pa}\cdot\text{m}^3\cdot\text{s}^{-1}$ will require a total pumping speed of the order of $300\,000 \text{ l}\cdot\text{s}^{-1}$.

Various pumping systems are being studied at present. The requirements are an ultimate operating pressure of 1×10^{-5} Pa, a roughing time of about 1 hour and, after initial outgassing, the operating pressure should be reached in about 20 hours. The pressure in the SSC will be reduced in three stages. Roughing from 10^5 to 10^2 Pa will be done by rotary vane pumps with a total pumping speed of about $500 \text{ m}^3\cdot\text{h}^{-1}$. Four turbomolecular pumps, each having a pumping speed in the range 2000 to $5000 \text{ l}\cdot\text{s}^{-1}$, will be used to reduce the pressure from 10^2 to 10^{-3} Pa. Eight cryopumps (20K refrigerator type), each having a pumping speed of about $40\,000 \text{ l}\cdot\text{s}^{-1}$, will be used for reducing the pressure from 10^{-3} to 10^{-5} Pa.

Small turbomolecular pumps ($\sim 500 \text{ l}\cdot\text{s}^{-1}$) may be added to each of the four transmission lines to pump the volumes behind the shorting plates. A quadrupole residual gas analyser will be fitted to the SSC for leak detection and residual gas analysis during operation.

The Central Region of the SSC

The pre-accelerated beam is injected radially through a valley in which it is bent through 4° by the stray sector magnet field before it enters the first bending magnet BM1 in the central region. Figure 8 shows the layout of this region. The beam is directed into a second bending magnet BM2 which deflects it by 95° into a magnetic inflection channel MIC in the pole tip of a sector magnet. A horizontal beam scanner mounted in

the valley vacuum chamber locates the beam in front of BM1 while a profile monitor determines the spatial beam distribution and the beam position in front of BM2.

BM1 and BM2 produce field strengths of 0,63 T and 1,6 T respectively. Both magnets allow for a beam height of 36 mm and a beam width of 100 mm. BM1 should be installed as close as possible to the vacuum chamber from which the beam emerges in order to control the beam as soon as it enters the central region. BM2 should be positioned as near to the free-valley vacuum chamber as is physically and magnetically feasible in order to reduce the MIC field and thus decrease its current and cooling requirements.

The minimum orbit separation at the exit of the MIC is 43 mm for an 8 MeV proton beam. The radial displacement between centred orbits for 8 MeV protons and heavy ions is approximately 44 mm at the MIC exit which implies that the MIC should be radially adjustable by 70 mm at this point. At the entrance an adjustment of only 10 mm is required. These requirements can be satisfied by rotating the MIC around a pivot point near its entrance. The MIC is 50 mm wide, 44 mm high and has a radius of curvature of 0,36 m. It increases the flux density in the pole tip by 0,15 T. A beam height of 26 mm and a beam width of 20 mm are allowed. The vertical and horizontal acceptances are 632 and 404 mm.mrad respectively.

Detailed designs of BM1, BM2 and the MIC have been made.

Beam Extraction from the SSC

With the relatively low sector-magnet field of 1,265 T and the large energy-gain per turn of 1 MeV at extraction, the orbit separation is approximately 7 mm for 200 MeV protons. Consequently we do not envisage employing resonances to enlarge this orbit separation. Extraction is accomplished with an electrostatic extraction channel and two septum magnets in succeeding valleys.

The estimated maximum permissible beam phase-width without flat-top acceleration is 8° before multi-turn extraction commences. It is therefore essential that the initial increase in orbit separation is realized by means of an electrostatic channel with a very thin molybdenum septum. This 50 cm long channel, with an electrostatic field strength of 50 kV/cm in the 15 mm wide gap, is located alongside the flat-top resonator and the opposite free valley is used to complete the extraction. It is placed in the second rather than the first half of the valley as its entrance should be at close to the point where the ratio of turn spacing to beam width is the largest. The radial and axial acceptances of this channel are 53 mm.mrad and 221 mm.mrad, respectively.

In order to ensure a large enough beam separation at the entrance to the second septum magnet for the radial focussing frequencies of all particle beams, a small (15 kg) septum magnet is placed inside one of the main resonators. This first 30 cm long septum magnet, with a septum thickness of 2 mm and a maximum flux density of 0,04 T, will give the beam a further outward deflection to ensure an orbit separation of at least 25 mm at the entrance to the second septum magnet. The latter has a length of 50 cm, a septum thickness of 15 mm, and can operate at fields up to 1,0 T. The field falls off quite rapidly outside these septum magnets. The radial and axial acceptances of both septum magnets are 212 mm.mrad and 221 mm.mrad, respectively. Final deflection out of the valley is accomplished with a C-shaped 1,6 T bending magnet.

The RF System

The main characteristics of the resonators are summarized

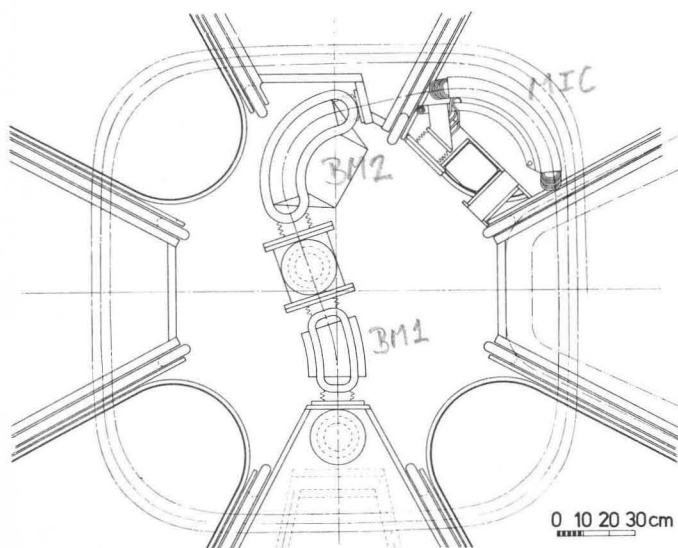


Fig. 8: Central region of the SSC

in table 2. Each of the two delta-type resonators is driven by a power amplifier through a capacitive coupling system.

Table 2: Characteristics of the Resonators

Number and Type	2 × 49° deltas, λ/2
Frequency Range	5 - 26 MHz
Tuning	Movable short, var. cap.
RF Power Consumption	2 × 75 kW
Dee Voltage	250 kV
Maximum Current Density	45 A/cm (peak)
Q-value	19 000
Accelerating Gap	100 mm
Resonator Angle	49°
Coupling System	capacitive

The position of the junction point between the inner conductor of the coaxial line and the delta is critical in determining the voltage distribution along the accelerating gaps at higher frequencies. The position of the line was optimised by means of measurements on a model. At 26 MHz the rf field at injection is 80% of the field at extraction. The current-density distribution in the outer delta chamber was measured on the same model. The electrical design of the resonator has been completed and the mechanical design is in progress.

A simplified diagram of the resonator is shown in figure 9. Each short-circuiting plate is adjusted by means of three telescopic lead-screws coupled together by a chain driven by a single motor. Retractable fingers are used to make contact on the inner and outer

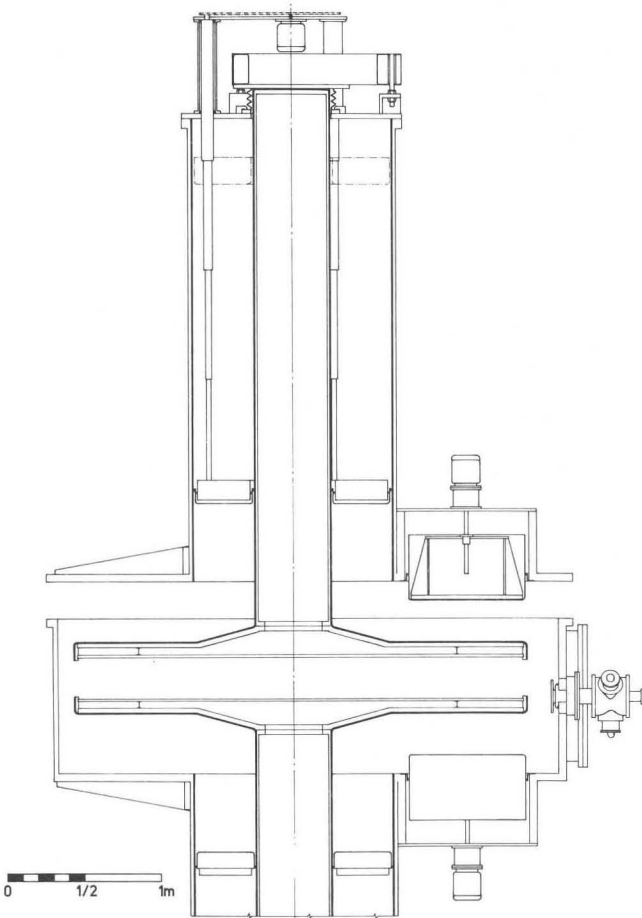


Fig. 9: Section through SSC resonator

conductors of the line. Each of the variable capacitors is adjustable from a position flush with the delta chamber to a position 15 mm from the delta surface.

It is intended to make each half of the delta and its associated inner conductor a mechanical unit. The copper surface of each inner conductor will be welded to the copper surface of the delta. The supporting structure will be bolted together. The outer conductors of the lines and the delta chamber will also be welded together except for the bolted junction between the delta chamber and its top cover plate, as shown in figure 9.

The characteristics of the power amplifiers have been specified and quotations invited and received. The first power amplifier will be procured early in 1979.

The Control System

A study of the requisites and design of a control system has shown that an estimated 3000 parameters will need to be monitored or controlled. These parameters can be classified into three groups associated with the injector cyclotrons, the SSC and the external beam facilities. The proposed control system comprises five 16-bit mini-computers, a CAMAC interface system between the computers and accelerator instrumentation, and a man-machine communication system (MMC). The five computers will operate in a hierarchical structure of two senior-level and three junior-level processors. The tasks to be performed by the senior computers include job scheduling and the provision of programs for the junior-level computers, the analysis of alarm conditions, data logging and communication with the MMC via CAMAC. The three junior-level computers will each monitor and control one of the three above-mentioned groups of parameters by means of three CAMAC parallel branch highways. To reduce cabling costs the junior-level computers will be located near the relevant instrumentation, and will communicate with the senior-level computers via serial co-axial cable links.

The CAMAC branch drivers, parallel branch highways, crates and (modified type-A) crate controllers to be used in the control system are components which differ slightly from the ESONE EUR 4600 standards, but give quicker LAM source identification and DMA data transfer and permit several branch drivers to multiplex onto one branch highway. Moreover, individual crates can be controlled both by the crate controller placed in the right-most crate position, and by autonomous controllers placed in any position in the crate. These possibilities will be exploited to increase the reliability and speed of the control system.

A computer-based CAMAC control system for the magnetic field measuring equipment is under construction at present.

Shielding

For the energy range of the SSC, the thickness of shielding material required at any place is determined by the secondary neutrons produced by the beam striking any object. This shielding will be more than enough to attenuate the gamma rays produced to an acceptable level. The shielding material considered is ordinary concrete, as this is relatively simple to cast either in situ or into movable wall blocks and beams. (Iron-ore aggregate for heavy concrete proves to be very expensive).

We calculate that the beam dumps for 1 μA beams of 200 MeV protons will require a minimum of 5.7 m of concrete in the forward direction from the end of the beam pipe, and 2.5 m in the backward direction.

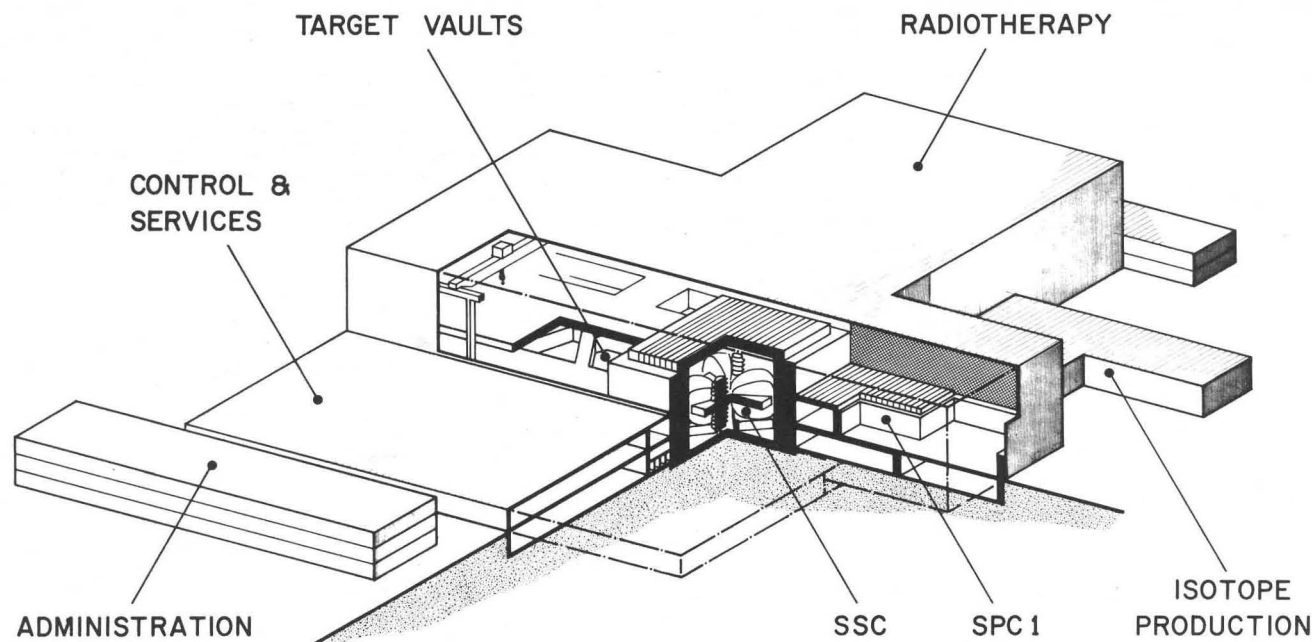


Fig. 10: Schematic drawing of the cyclotron complex

For shielding of the cyclotron itself, 4.3 m of ordinary concrete will provide sufficient shielding for up to 10 μ A of 200 MeV protons: an acceptable beam loss will normally be only about 10% of the total beam and this, together with the fact that the cyclotron will be self-shielding to some extent, will reduce the neutron flux to an acceptable level. Where high losses may occur, such as at the various deflector stages (septa), local shielding can also be used if this proves to be necessary.

Where possible, movable wall blocks will be used, and all overhead shielding will consist of demountable concrete beams.

Buildings and Site

A design team has been set up to co-ordinate the design and siting of the accelerator complex. The team consists of the Head and representatives of the NAC, the CSIR Estates Department, structural engineering consultants, mechanical and electrical consultants, architectural consultants, and a firm of quantity surveyors.

For design purposes the complex has been divided into two sections. The first comprises the core of the facility, i.e. the cyclotron hall including the experimental area, isotope production vaults, radiotherapy vaults and the "control and services" section adjacent to the cyclotron hall. The second section consists of the office and laboratory accommodation, radiotherapy areas beyond the therapy vaults, isotope-handling laboratories etc.

Figure 10 gives some idea of the scale of the project: the cyclotron hall will be of the order of 24 m high, as an overhead crane with a 60 t lifting capacity must be provided with sufficient clearance above the walls of the cyclotron vault to permit the sections of the sector magnets and resonators to be lifted out. Additional cranes of smaller capacity are also needed to remove roof beams and to position beamline components for the radiotherapy and isotope vaults, and for the beam corridor.

Alternative layouts, of which many have been studied, suffer from increased beamline costs and a lack of accessibility to the various target points. Some fairly detailed planning has been attempted for areas such as the control and services area, and the multi-storey office and laboratory block for administrative and technical support personnel, but no final drawings have yet been prepared.

The site chosen is 33 km from the centre of Cape Town and approximately 30 km by road from both Groote Schuur Hospital and Tygerberg Hospital. The 35 ha. site is adjacent to the 6 MV Van de Graaff accelerator of the Southern Universities Nuclear Institute, and 20 km from the D F Malan International Airport. The site is virtually flat with sound rock at 30 m below the surface. The upper 7 m is sand and calcrete, underlain by weathered shale and clay seams. The presence of the clay layer necessitates founding of the accelerator on the sound rock in order to avoid excessive settlement. A large number of deep piles will therefore be required. A possible problem is the variable water table, which is known to rise almost to the surface in winter: special provision will be made for waterproofing and drainage of the basement areas.

References

1. W L Rautenbach and A H Botha, Proposal for a South African National Accelerator Facility, Proceedings of the Seventh International Conference on Cyclotrons and Their Applications, (Birkhäuser, Basel 1975), p.117 - 120.
2. Technical Report of the Accelerator Task Group, National Accelerator Project, Pretoria (1976).
3. A H Botha et al., A New Multi-Disciplinary Separated-sector Cyclotron Facility, IEEE Trans. NS-24, No. 3 p. 1118 - 1120 June 1977.
4. Annual Report of the National Accelerator Centre, National Accelerator Centre, Stellenbosch (1978)
5. F J Mumford et al., Design of a Vacuum Chamber for the Magnets of a Separated-Sector Cyclotron. This conference.

** DISCUSSION **

W. JOHO: For medical therapy with neutrons, do you plan to use the proton or the deuteron beams?

A. BOTHA: We shall use proton beams.

F. RESMINI: What is the trim coil power anticipated for the separated sector cyclotron?

A. BOTHA: We have not yet designed the trim coils in detail. The power consumption will be approximately 100 kW. We are operating at a very low flux density (maximum 1265 tesla), so the umbrella effect at minimum and maximum radii is not very strong.

J. RICHARDSON: What will be the cost of the facility?

A. BOTHA: The total cost is of the order of \$28 million dollars.